# NATIONAL ADVISORY COMMITTEE FOR AERONAUTICS

TECHNICAL NOTE 3870

MEASUREMENT OF THE LONGITUDINAL MOMENT OF INERTIA

OF A FLEXIBLE AIRPLANE

By Henry A. Cole, Jr., and Frances L. Bennion

Ames Aeronautical Laboratory Moffett Field, Calif.



Washington November 1956 TECHNICAL NOTE 3870

MEASUREMENT OF THE LONGITUDINAL MOMENT OF INERTIA

OF A FLEXIBLE AIRPLANE<sup>1</sup>

By Henry A. Cole, Jr., and Frances L. Bennion

#### SUMMARY

The method of measuring moment of inertia of an airplane by oscillating it on knife edges and a spring is examined analytically for application to flexible airplanes. First, the equations of motion of a flexible airplane mounted on three supports are presented. Then these equations are examined for conditions required to minimize the difference between the apparent inertia of the flexible airplane and the inertia of the rigid airplane. The analysis is applied to a flexible airplane mounted on various combinations of springs and knife edges. A practical combination is then selected in which the moment-of-inertia correction for flexibility is very small.

The application and results of the above method in ground oscillation tests are described. The various corrections to reduce the measured moment of inertia to the reference axis moment of inertia are presented. The results show that measurement of moment of inertia by this method is practicable, provided the knife edges and spring are arranged to minimize excitation of structural modes.

#### INTRODUCTION

In the evaluation of stability derivatives from dynamic flight-test data and in the prediction of the dynamic stability and control of an airplane, accurate values of the moment of inertia are important. Estimates of moment of inertia are usually of doubtful accuracy because of the large number of parts in an airplane; hence, it is desirable whenever possible, to measure moments of inertia. Although moment of inertia is a property of rigid bodies, it is used in dynamic stability calculations for flexible airplanes because inertial effects due to flexibility are usually insignificant near frequencies of the airplane oscillatory modes. For frequencies near the structural modes, inertial effects due to flexibility have to be taken into account in the analysis.

<sup>&</sup>lt;sup>1</sup>Supersedes recently declassified RM A55J2l by Henry A. Cole, Jr., and Frances L. Bennion, 1956.

The present investigation was conducted to obtain reliable measurements of longitudinal moment of inertia of a large flexible swept-wing airplane for use in conjunction with the dynamic stability and control program which is reported in reference 1. The airplane was oscillated on a support of a spring and two knife edges because this appeared to be most practical for a large airplane. This method is commonly used for the determination of moment of inertia of rigid airplanes (ref. 2). Design of the support equipment becomes more critical for a flexible airplane because dynamic coupling of airplane structural modes with the support spring system can cause serious errors in the measured frequency from which the moment of inertia is calculated. Furthermore, the loads at the three supporting points may be near the maximum allowable; hence, additional loads due to dynamic forces may overstress the airplane structure. In order to overcome these difficulties, the spring-airplane dynamic systems for a wide range of spring and knife-edge arrangements were analyzed, and a combination was selected which practically eliminated the effects of structural flexibility.

The methods used in the dynamical-systems studies and the results should be of general interest because they may be applied to other airplanes in which flexibility is a problem. The first part of the report presents methods which can be used to minimize the effects of flexibility. The second part deals with ground oscillation tests of the airplane conducted by personnel of the High-Speed Flight Station of the NACA at Edwards Air Force Base, California.

#### NOTATION

- aij system influence coefficient, deflection at station i, relative to horizontal plane, due to load at station j, in./1000 lb
- wing influence coefficient, deflection at station i, relative to fuselage center line, due to load at station j, in./1000 lb (Because of symmetry, stiffness of both wings is included.)
- i,j arbitrary station numbers
- k spring constant, 1000 lb/in.
- m<sub>i</sub> equivalent mass at station i, slugs
  (Because of symmetry, mass of both wings is included in wing stations.)
- r knife-edge station (station 3 for the test location and station 3' for the alternate location)
- x longitudinal distance from knife edge, in.

NACA IN 3870

3

xi longitudinal distance of station i from knife-edge axis, in.

- xs longitudinal distance of spring from knife-edge axis, in.
- z vertical distance from the horizontal plane through the knife-edge axis, in.
- zi vertical displacement of station i relative to horizontal plane through knife-edge axis, in.
- Fi vertical force at station i, lb
- IA apparent moment of inertia, slug-ft<sup>2</sup>
- IF fuselage moment of inertia, slug-ft<sup>2</sup>
- Iw wing moment of inertia, slug-ft2
- Iy longitudinal moment of inertia, slug-ft2
- Iyref longitudinal moment of inertia about the body reference axis passing through the airplane center of gravity, slug-ft<sup>2</sup>
- δ perpendicular distance from plane passing through wing chord at wing-fuselage juncture, in.
- displacement of station i relative to a plane passing through wing chord at wing-fuselage juncture, in.
- displacement of knife edges from plane passing through wing chord at wing-fuselage juncture, in.
- $\theta$  angle of rotation of fuselage center line, radians
- ω frequency, radians/sec
- wn undamped natural frequency of flexible airplane in test rig, radians/sec
- $\omega_{n_1}$  wing first-bending mode frequency, radians/sec
- wo undamped natural frequency of rigid airplane in test rig, radians/sec

#### Matrices

{ } column matrix
 square matrix

- L] row matrix
- $[^{\circ}]$  square matrix with all except diagonal elements equal to zero
- [ ]' transposed matrix
- [1] unit matrix, matrix which has units for all of its principal diagonal elements and zeros for the remainder of its elements
- $\{1\}$  column matrix with all elements equal to 1
- [1] row matrix with all elements equal to 1

#### ANALYSIS OF PROBLEM

The basic problem was to devise a method to measure moment of inertia of a flexible airplane. The moment of inertia of rigid airplanes is usually obtained by measuring the frequency of the airplane when oscillated on a pair of knife edges and restrained by a spring. When this method is applied to a flexible airplane, the structural modes can couple with the supporting spring reaction forces so that simple calculations of moment of inertia from the measured frequency are no longer valid. Corrections for the effect of structural modes on the measured frequency requires knowledge of the structural deflections (modes) and spring constants, or spring constants and mass distribution of flexible parts; usually these are not known accurately. A more practical approach is to seek methods in which flexibility effects on the measured frequency are small. Approximate equations for the airplane dynamic system supported by knife edges and a spring will be developed first, and then the application of these equations to the test airplane will be made to determine practical methods for measuring the moment of inertia.

## Airplane-Support Dynamic Equations

The airplane and support system may be approximately represented by a system of discrete masses elastically connected as shown in figure 1. The selection of the distribution and number of masses is discussed in reference 3. In general, mass points are selected for all relatively rigid masses on the airplane such as the fuselage and nacelles. Then the distributed mass of the flexible parts is divided into segments, which should be increased in number as more accuracy is desired. The accuracy of a particular discrete mass arrangement can be checked by comparing the

deflections of the elastic system under inertial loadings of the discrete masses and of the continuous mass for the mode of interest.

If the angle  $\theta$  is assumed small in the coordinate system of figure 1, then only the vertical displacements,  $z_i$ , of the mass points need to be considered in the equations of motion. The spring characteristics can be conveniently expressed in the form of influence coefficients,  $a_{ij}$ , which represent the deflection at station i due to a unit load at station j. The influence coefficients can either be calculated or measured directly on the airplane-support system.

The deflection at the mass points in terms of the applied forces is given by:

$$z_{1} = \frac{1}{1000} \left( a_{11}F_{1} + a_{12}F_{2} + a_{13}F_{3} \dots + a_{1N}F_{N} \right)$$

$$z_{2} = \frac{1}{1000} \left( a_{21}F_{1} + a_{22}F_{2} + a_{23}F_{3} \dots + a_{2N}F_{N} \right)$$

$$z_{N} = \frac{1}{1000} \left( a_{N1}F_{1} + a_{N2}F_{2} + a_{N3}F_{3} \dots + a_{NN}F_{N} \right)$$
(la)

These equations can be more conveniently written in matrix form as follows:

$$\{z_i\} = \frac{1}{1000} [a_{i,j}] \{F_i\}; i, j = 1, 2, ..., N$$
 (1b)

Matrix notation will be used throughout the remainder of the report. These equations can easily be converted to tabular form by applying the rules of matrix multiplication, addition, and transposition which are explained in Chapter 1 of reference 4.

Oftentimes, the influence coefficients of the airplane wing are known relative to the fuselage ( $\delta$  coordinates in fig. 1). If these are expressed in matrix form  $[b_{ij}]$  where the element  $b_{ij}$  is the deflection at station i, relative to fuselage, due to a load at station j, then the influence coefficients  $[a_{ij}]$  for equation (1b) may be obtained by the following transformation

$$\begin{bmatrix} \mathbf{a}_{ij} \end{bmatrix} = \begin{bmatrix} \mathbf{c} \end{bmatrix} \begin{bmatrix} \mathbf{b}_{ij} \end{bmatrix} \begin{bmatrix} \mathbf{c} \end{bmatrix}' + \frac{1}{k} \left\{ \frac{\mathbf{x}_{i}}{\mathbf{x}_{s}} \right\} \begin{bmatrix} \frac{\mathbf{x}_{i}}{\mathbf{x}_{s}} \end{bmatrix}; \quad i, j = 1, 2, \dots, \mathbb{N}$$
 (2)

where

[c] = [l] + 
$$\begin{bmatrix} 0 & 0 & \cdots & \left(\frac{x_1}{x_S} - 1\right) & \cdots & 0 \\ 0 & 0 & \cdots & \left(\frac{x_2}{x_S} - 1\right) & \cdots & 0 \\ \vdots & \vdots & \ddots & \vdots & \vdots \\ 0 & 0 & \cdots & \left(\frac{x_N}{x_S} - 1\right) & \cdots & 0 \end{bmatrix}$$

and r represents the station where the knife edges are located. This equation is derived in Appendix A.

For sinusoidal motion, the inertial force applied to the structure is  $F_i = \frac{1}{12} \omega_n^2 z_i m_i$ . Then

$$\left\{z_{i}\right\} = \frac{1}{12000} \omega_{n}^{2} \left[a_{i,j}\right] \left[m_{i}\right] \left\{z_{i}\right\}; \quad i,j = 1,2,\ldots,N$$
 (3)

The modes and natural frequencies of this dynamic system may be determined by solving equation (3) by methods described in reference 4. Since the fundamental mode is the only one used to determine the moment of inertia, the simple iteration solution of equation (3) is most practical. Assume a modal column, z  $z_i$ , substitute into the right-hand side of equation (3), and perform the indicated matrix multiplications. The resulting modal column is normalized and again substituted into the right-hand side of equation (3). This process is repeated until successive normalized modal columns are equal. The inverse of the normalizing multiplier is the frequency squared.

The rigid airplane can be treated as a special case of equation (3) in which the  $[b_{ij}]$  part of  $[a_{ij}]$  is equal to the zero matrix. Then by equations (2) and (3)

<sup>&</sup>lt;sup>2</sup>A modal column is a set of coordinates which describes the characteristic shape in which the system oscillates.

NACA IN 3870

and, since  $\{z_i\}$  is invariant for the rigid case, equation (4a) reduces to the well-known equation for a rigid airplane:

$$\omega_0^2 = \frac{12000 \text{ kx}_S^2}{\sum_{i=1}^{N} m_i x_i^2}$$
 (4b)

from which the moment of inertia is obtained:

$$I_{y} = \sum_{i=1}^{N} \frac{m_{i}x_{i}^{2}}{144} = \frac{1000 \text{ kx}_{s}^{2}}{12 \omega_{o}^{2}}$$
 (4c)

### Minimization of Flexibility Effects

The practical frequencies for ground oscillation tests to determine moment of inertia naturally fall below the frequencies of the structural modes. Also, frequencies near zero are not practical because of the large static spring deflections required and the relatively larger effect of friction and damping forces. Hence, the highest frequency at which flexibility effects are small is probably the most desirable. Several approaches are available. One is to select locations of knife edges and springs which suppress or uncouple the lowest airplane structural mode, thus raising the available band of frequencies in which flexibility effects are small. Another approach is to limit the frequency to values which keep flexibility effects small. Discussion of these approaches follows.

Uncoupling of the wing first-bending mode .- When the airplane is oscillated at frequencies below the structural-mode frequencies, the inertial forces in the wing excite the wing first-bending mode primarily. The degree of excitation will, of course, depend on the location of the rotational axis and the frequency. Although it is possible to solve for an axis which gives the minimum excitation to the wing, the choice of the axis is usually restricted to some point near the center of gravity if static spring deflections are to be kept within practical limits. Since the axis of rotation is more or less fixed, an external force is needed to suppress the wing first-bending mode. Such a force is available in the reaction force at the knife edges if they are located out on the wing. The problem then resolves itself into one of selecting a spring location which gives the reaction force the amplitude and phase necessary to cancel out the major part of the wing first-bending mode. Since the principal masses are located in the fuselage, a good criterion to optimize the spring location is to minimize the deflection of the fuselage relative to the

NACA TN 3870

knife edges  $(\delta_r)$ . This imposes boundary conditions similar to those of a rigid strut from the wing to the fuselage. The minimum value of  $\delta_r$  can be determined by solving for  $\left\{z_i\right\}$  over a range of  $x_s$ , calculating  $\delta_r$  from  $\left\{z_i\right\}$  and plotting versus  $x_s$ .

Cases where uncoupling is not practical. In some cases it will not be practical to locate knife edges sufficiently far out on the wing to uncouple the wing first-bending mode. In such cases flexibility effects can be kept small only by keeping the frequency small. A simplified analysis (Appendix B) of a swept-wing configuration in which the knife edges are located near the wing root shows that the apparent inertia is:

$$I_{A} = I_{F} + \frac{I_{W}}{1 - (\omega_{O}/\omega_{n_{1}})^{2}}$$
 (5)

The moment of inertia of the wing,  $I_W$ , is usually about 15 percent of the total moment of inertia when nacelles are located near the wing tips. Then, according to equation (5), errors in moment of inertia greater than 5 percent will be caused by flexibility if  $\omega_O$  is greater than 50 percent of  $\omega_{n_1}$ .

### Analysis of Test Airplane

The dynamic-analysis techniques just described were applied to a test airplane which was represented by discrete masses as shown in figure 2. The airplane dimensions are given in table I and estimated masses and influence coefficients are given in table II obtained from references 1 and 5. Combinations of spring and knife-edge locations as shown on figure 3 were considered. The most practical combinations are those of figures 3(a) and 3(b) because the knife edges are near the center of gravity which gives small static spring deflections and the compression springs reduce the load at the knife edges. The combination of figure 3(c) was considered because it is an arrangement which is sometimes used on rigid airplanes and provides an interesting comparison with the arrangement of figure 3(a) since the reaction forces of the two springs are 180° out of phase.

Through use of equations (3) and (4b) the frequencies for the flexible and rigid airplane were calculated for the combinations of figure 3. The results are shown for a range of spring constants on figure 4. The frequency of the flexible airplane using the combination of figure 3(a) is nearly the same as the frequency of the rigid airplane but the combinations of figures 3(b) and 3(c) show large shifts in frequency due to flexibility for constant k. Hence, the arrangement shown on figure 3(a) is the most desirable of the three from the standpoint of reducing flexibility effects.

The reason for the large shifts in frequency is indicated by the corresponding modes,  $\{z_i\}$ , plotted in figure 5. This figure shows the relative movement of the fuselage and wing when they oscillate in the fundamental mode. The modes have been normalized to the same angle of rotation so that the relative amounts of wing deflection are apparent. It may be seen that system (a) oscillates very nearly as a rigid airplane in contrast to systems (b) and (c) which have relatively large wing deflections.

Although the fuselage jack points are the most practical locations for the spring, it is interesting to estimate the optimum location. Figure 6 shows the variation of the deflection of fuselage relative to knife edges,  $\delta_{\rm r}$ , with spring location,  $x_{\rm s}$ . The deflection goes to zero at  $x_{\rm s}=0$  and  $x_{\rm s}=680$  inches which is at the nose of the airplane and is noted on figure 2. The former value is trivial because frequency is zero at this point, but the latter value indicates the approximate spring location to minimize flexibility effects.

A direct indication of the effects of flexibility on the measured moment of inertia is obtained by calculating the square of the ratio of the flexible to rigid airplane frequencies,  $(\omega_{\rm D}/\omega_{\rm O})^2$ . This parameter is inversely proportional to the ratio of the flexible airplane apparent moment of inertia and the rigid airplane moment of inertia. Variation of this parameter for the two knife-edge locations and a range of spring locations is shown in figure 7. The difference of the values from 1.00 indicates the error in moment of inertia which would result if flexibility were not taken into account. With knife edges at the inboard wing jack points, the optimum location of the spring is at  $x_s = 0$ , but this location is impractical because the frequency is zero. As xs is increased or decreased, the inertia parameter falls off rapidly. On the other hand, the inertia parameter for the system with knife edges at outboard wing jacks shows an initial increase in accuracy with xs and does not fall off until considerably higher values of xs are reached. It is interesting to note that the optimum value for the outboard wing-jack system is near the point for  $\delta_r = 0$  which supports the use of this criterion to estimate the optimum.

The degree of coupling of the rigid airplane mode and the wing first-bending mode is indicated by the variation of the inertia parameter,  $(\omega_n/\omega_0)^2$ , as the frequency of the rigid airplane approaches the wing first-bending mode frequency of 7.3 radians per second. The two frequencies become equal for the spring location of  $x_{\rm S}=830$  and a spring constant of 1.132. As indicated on figure 7, the outboard wing-jack system incurs an error of only 3 percent in the inertia parameter, indicating a small amount of coupling as compared to 19 percent for the inboard wing-jack system, indicating a large amount of coupling.

## MEASUREMENT OF MOMENT OF INERTIA

## Test Equipment

The knife-edge and spring combination of figure 3(a) was selected for use on the test airplane because it satisfied the practical considerations of small static spring deflections and simplicity of attachments to jack points and at the same time would only cause an estimated 2.4-percent change in the inertia due to flexibility. Knife-edge and spring installation details are shown on figures 8 and 9. The spring was calibrated by applying a load with a hydraulic press and loads were measured with a strain-gage load instrument. The spring was preloaded to 10,000 pounds prior to the test to simplify setting up the static spring deflection (10 in.) for the test configuration. The airplane was equipped with an optigraph, developed by the NACA, which records the motion of 100-watt target lights on the wing and fuselage. For this test, target lights were also mounted on a stand near the tail to give a horizon reference. The location of target lights used in this report is indicated in figures 2 and 3(a). A control position recorder was also installed to indicate spring deflections.

## Experimental Procedure and Measurements

The airplane was weighed in the defueled condition on the outboard wing jacks and the front fuselage jack point. The airplane was weighed at the points of support of the spring and knife edges in order to check the loads on the test equipment and airplane structure. Gross weight was 81,390 pounds with center of gravity located at 13.6-percent mean aerodynamic chord. In this condition it was estimated that the static spring deflection would be too large so 500 pounds ballast was added to the tail. Then the total static load on the spring was 11,520 pounds.

The airplane was raised with the outboard wing jacks, with knife edges installed, until the rear wheels cleared the floor by 3 inches. Then the nose was raised by the inboard wing jacks until the spring shaft could be moved into place under the forward fuselage jack point. The inboard wing jacks were then lowered and removed so that the airplane rested only on the knife edges and the spring. The wheels were left down for safety.

Oscillations were excited by hand and the subsequent free oscillations of wing and body were measured by the optigraph. Unfortunately, the control position recorder malfunctioned, but it was felt that the optigraph records were sufficient. Typical time histories of the optigraph measurements are shown on figure 10. It is apparent from the wingtip records that modes other than the fundamental were excited. Also, it

NACA TN 3870

should be noted that the deflections at the wing tip were extremely small and on the fringe of measuring accuracy of the optigraph as indicated by the small deflection of the traces (0.005-in. trace deflection on the photographic film). A discussion of these higher modes follows.

Effect of subdominant structural modes. Several analyses were made to determine the distortion of the time histories from the fundamental mode caused by the higher-frequency modes. A dynamic analysis of the subdominant modes (ref. 4) was carried out and the results are shown on figure 11. In this figure the modal columns of the first three subdominant modes are plotted. In every case the deflection of the wing tip is greater than the deflection at the tail. Hence, since the wing-tip deflections were barely measurable, the distortion of the horizon target trace (fig. 10) by these higher modes is negligible. This result was verified by the horizon-target time histories. Components of the calculated modes were found to be present but they were too small to affect the measured frequency of the fundamental, especially since an average was taken over a large number of cycles.

#### Reduction of Data

The average period of the horizon-target deflection oscillation was determined from 24 cycles and estimated accuracy is 3 percent. Measurements and corrections are as follows:

Period = 1.70  $\pm$ 0.05 sec  $\omega_n$  = 3.70  $\pm$ 0.13 radians/sec k = 1.132 1000 lb/in.  $x_s$  = 391.4 in.

From equation (4c), the measured moment of inertia is obtained

 $I_y = 1,056,000 \text{ slug-ft}^2$ 

Correction for flexibility.— The test frequency of 3.7 radians per second very nearly corresponds to the frequency shown in figure 4 (curve labeled 3(a) for k=1.132 and  $x_S=391.4$ ). For these conditions the inertial parameter determined from figure 7 is 97.6; hence, the correction for flexibility is 2.4 percent or -25,000 slug-feet squared.

Correction for additional apparent mass. - Additional apparent mass was calculated by the method of reference 6 and the correction was found to be -20,800 slug-feet squared.

Correction to center of gravity. The correction for transfer of moment of inertia from knife edge to center of gravity is -65,500 slugfeet squared.

Correction for ballast and pilots. The correction to subtract the moment of inertia of the 500-pound ballast and to add pilots (400 pounds) to the airplane gave -26,900 and +15,200 slug-feet squared, respectively.

Friction and damping. - The effect of friction and damping on the measured frequency was estimated and found to be negligible.

Wheels.- Although the wheels were down during the tests, calculations indicated that the difference between moment of inertia with wheels up and wheels down was negligible.

Summary of corrections and moment of inertia.— The measured moment of inertia and corrections are summarized below. From these values the longitudinal moment of inertia about the reference axis is obtained for the airplane ready to fly except for fuel (81,790 pounds, center of gravity = 12.4-percent mean aerodynamic chord).

	slug-ft <sup>2</sup>
Measured Iy	1,056,000
Flexibility	<b>-</b> 25 <b>,</b> 000
Additional apparent mass	-20,800
C.G. transfer	<b>-</b> 65 <b>,</b> 500
Ballast	<b>-</b> 26,900
Pilots	+15,200
Iyref	933,000

It is interesting to note that the correction for flexibility is only 2.4 percent as compared to the total correction of 14.5 percent of measured  $I_{\rm V}$ .

#### CONCLUSIONS

Analytical and experimental evaluation of ground oscillation tests to measure the longitudinal moment of inertia of a large flexible airplane has led to the conclusion that practicable and accurate measurements of the longitudinal moment of inertia of large flexible airplanes can be made

NACA IN 3870

by oscillating the airplane on a set of knife edges and a spring, which are arranged so as to minimize excitation of structural modes. The effects of flexibility on the fundamental frequency can be minimized by reducing the coupling between the spring system mode and the airplane first-bending mode. This can be done by locating the knife edges outboard on the wing and selecting a spring location such that the reaction forces tend to cancel out the wing first-bending mode. For cases where it is not practical to locate the knife edges outboard on the wing, analyses indicate that the fundamental frequency should be small relative to the lowest structural mode frequency (less than 50 percent) to avoid excessive errors in measured moment of inertia.

Ames Aeronautical Laboratory
National Advisory Committee for Aeronautics
Moffett Field, Calif., Oct. 21, 1955

#### APPENDIX A

## DERIVATION OF AIRPLANE-SUPPORT INFLUENCE COEFFICIENTS

The coordinate system used in this analysis is shown in figure 1. Assume that the airplane influence coefficients are known for the mass stations and the knife-edge location; that is, [bij] is known in the equation:

$$\left\{\delta_{i}\right\} = \left[b_{i,j}\right] \left\{F_{i}\right\} \tag{Al}$$

where i = 1, ..., N and r represents the station of the knife edges.

The sum of moments about the reaction point, r, must be equal to zero. Hence:

$$\left| x_{i} \right| \left\{ F_{i} \right\} + x_{s}k(\delta_{r} - \theta x_{s}) = 0$$
 (A2)

The sum of the vertical forces must be equal to zero. Hence:

$$[1] \left\{ F_{i} \right\} + k(\delta_{r} - \theta_{x_{s}}) + R = 0 \tag{A3}$$

where R is the reaction force at the knife edge.

Combining equations (A3) and (A2) gives:

$$R = \left\lfloor \frac{x_{i}}{x_{s}} - 1 \right\rfloor \left\{ F_{i} \right\} \tag{A4}$$

Including the reaction force in equation (A4) with the applied forces in equation (A1) gives:

$$\left\{\delta_{i}\right\} = \left[b_{i,j}\right] \left[\left[1\right] + \left\{\begin{matrix} \circ \\ i \\ 0 \end{matrix}\right\} \left[\frac{x_{i}}{x_{s}} - 1\right]\right] \left\{F_{i}\right\} \tag{A5}$$

NACA TN 3870

where the 1 in the column matrix,  $\{i \}$ , appears in the rth row and all other elements are zero.

For small angles, the deflections zi can be obtained by:

By solving for  $\theta$  in equation (A2) and using equations (A5) and (A6), and noting that  $\delta_r = [0\ 0\ \cdot \cdot 1\ 0] \{\delta_i\}$  where the 1 occurs in the rth column, it may be shown that:

$$\left\{z_{i}\right\} = \left[\left[c\right]\left[b_{i,j}\right]\left[c\right]' + \frac{1}{k}\left\{\frac{x_{i}}{x_{s}}\right\}\left[\frac{x_{i}}{x_{s}}\right]\right]\left\{F_{i}\right\} \tag{A7}$$

where

$$[c] = [1] + \begin{bmatrix} 0 & 0 & \cdots & \left(\frac{x_1}{x_S} - 1\right) & \cdots & 0 \\ 0 & 0 & \cdots & \left(\frac{x_2}{x_S} - 1\right) & \cdots & 0 \\ \vdots & \vdots & \vdots & \vdots & \vdots \\ 0 & 0 & \cdots & \left(\frac{x_N}{x_S} - 1\right) & \cdots & 0 \end{bmatrix}$$

in which the  $\left(\frac{x_1}{x_S} - 1\right)$  terms appear in the rth column.

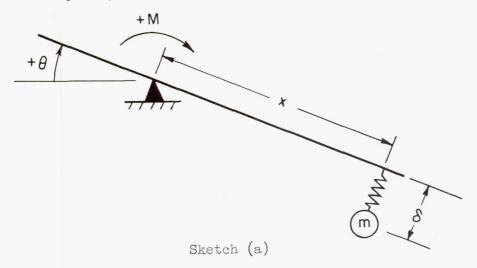
The influence coefficient matrix of the airplane supported on knife edges and springs is:

$$\begin{bmatrix} a_{i,j} \end{bmatrix} = \begin{bmatrix} c \end{bmatrix} \begin{bmatrix} b_{i,j} \end{bmatrix} \begin{bmatrix} c \end{bmatrix}' + \frac{1}{k} \begin{bmatrix} \frac{x_i}{x_s} \end{bmatrix} \begin{bmatrix} \frac{x_i}{x_s} \end{bmatrix}; \quad i,j = 1,2,\ldots, N \quad (A8)$$

#### APPENDIX B

## APPARENT INERTIA OF A MASS-SPRING SYSTEM

Consider a mass connected to a pivot point by a spring as shown in sketch (a). If a sinusoidal forcing moment, M, of frequency  $\omega$  is applied to the system, what is the apparent inertia?



The equations of motion neglecting gravity are:

$$mx^2\ddot{\theta} + mx\ddot{\delta} = M$$
 (B1)

$$mx\ddot{\theta} + m\ddot{\delta} + k_1\delta = 0$$
 (B2)

where

$$\ddot{\theta} = \frac{d^2\theta}{dt^2}$$
 and  $\ddot{\delta} = \frac{d^2\delta}{dt^2}$ 

Solving for the steady-state solution of  $\ddot{\theta}$  gives:

$$\ddot{\theta} = \frac{M}{mx^2 \left(\frac{1}{1 - \frac{m}{k_1} \omega^2}\right)}$$
 (B3)

and since the natural frequency is given by  $\omega_{n_1}^2 = k_1/m$  and the true moment of inertia by  $I = mx^2$ ; then

$$I_{A} = \frac{M}{\ddot{\theta}} = I \left[ \frac{1}{1 - \left( \frac{\omega}{\omega_{n_{1}}} \right)^{2}} \right]$$
 (B4)

When a fuselage-wing combination is oscillated at frequencies below the first-bending mode frequency, the wing-bending curve is very similar to that of the first-bending mode. Hence, this simple two-degree-offreedom analysis is approximately correct for a complete wing for frequencies below the wing first-bending mode. The apparent inertia of a rigid fuselage with a flexible wing attached is approximately given by

$$I_{A} = I_{F} + \frac{I_{W}}{1 - \left(\frac{\omega_{O}}{\omega_{n_{1}}}\right)^{2}}$$
(B5)

where

IA apparent moment of inertia

IF fuselage moment of inertia

 $I_{\overline{W}}$  wing moment of inertia

 $\omega_{\rm n}$ , wing first-bending mode frequency

#### REFERENCES

- 1. Cole, Henry A., Jr., Brown, Stuart C., and Holleman, Euclid C.:
  Experimental and Predicted Longitudinal Response Characteristics
  of a Large Flexible 35° Swept-Wing Airplane at an Altitude of
  35,000 Feet. NACA RM A54H09, 1954.
- 2. Turner, Howard L.: Measurement of the Moments of Inertia of an Airplane by a Simplified Method. NACA TN 2201, 1950.
- 3. Hunn, B. A.: A Method of Calculating the Normal Modes of an Aircraft. Quart. Jour. Mech. and Appl. Math., Mar. 1955, pp. 38-58.
- 4. Frazer, R. A., Duncan, W. J., and Collar, A. R.: Elementary Matrices.
  The MacMillan Co., 1946.
- 5. Mayo, Alton P., and Ward, J. F.: Experimental Influence Coefficients for the Deflection of the Wing of a Full-Scale, Swept-Wing Bomber.

  NACA RM L53L23, 1954.
- 6. Malvestuto, Frank S., Jr., and Gale, Lawrence J.: Formulas for Additional Mass Corrections to the Moments of Inertia of Airplanes. NACA TN 1187, 1947.

## TABLE I.- AIRPLANE DIMENSIONAL CHARACTERISTICS

		 				_		_	 	 	 	 	 _	
Fuselage Length, ft Average width, Average depth,	ft													6.95
Wing														
Span, ft Area, sq ft Aspect ratio . Taper ratio . Sweep angle (2) Dihedral angle		· ent	· ·		· · · · · · · · · · · · · · · · · · ·	,	de	·	 	 	 	 	 	9.43
Horizontal tail Area, sq ft . Aspect ratio .														268 4.06

TABLE II.- AIRPLANE MASS AND SPRING CHARACTERISTICS

(a) Mass distribution

1	Station													
	1	2	3	31	4	5	6	7	8					
mi	483.6	259.6	0	0	121.8	205.8	39.8	716.4	716.4					
Percent wing semispan	•383	.383	.400	.197	.707	•795	.924	0	0					
Percent wing chord	39	.38	.58	.58	.38	.14	.38							
Knife edges at outboard wing jack points														
xi	169.3	43.7	0		-109.5	-123.3	-211.5	384.9	-247.1					
Knife edges at inboard wing jack points														
xi	49.4	-76.2		0	-229.4	-243.2	-331.4	265.0	-367.0					

(b) Wing influence coefficients bij

								_	-
i	1	2	3	3'	4	5	6	7	8
1	0.0637	0.0175	0.0214	0.0055	0.0486	0.0722	0.0629	0	0
2	.0294	.0360	.0408	.0075	.0993	.1130	.1394	0	0
3	.0217	.0442	.0540		.1258	.1403	.1784	0	0
3'	.0019	.0082		.0032	.0164	.0162	.0225	0	0
14	.0622	.0993	.1209	.0164	.4103	.4820	.6530	0	0
5	.0764	.1105	.1330	.0180	.4770	.5948	.8217	0	0
6	.0803	.1288	.1603	.0224	.6421	.8218	1.2231	0	0
7	0	0	0	0	0	0	0	0	0
8	0	0	0	0	0	0	0	0	0

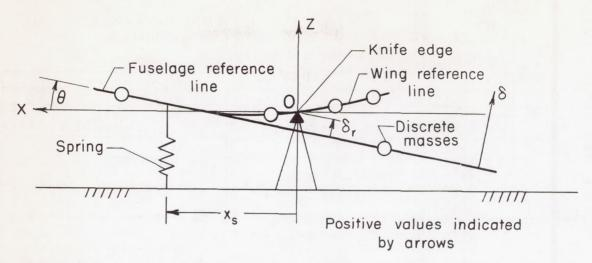


Figure 1.- Coordinate system (side view of airplane and support).

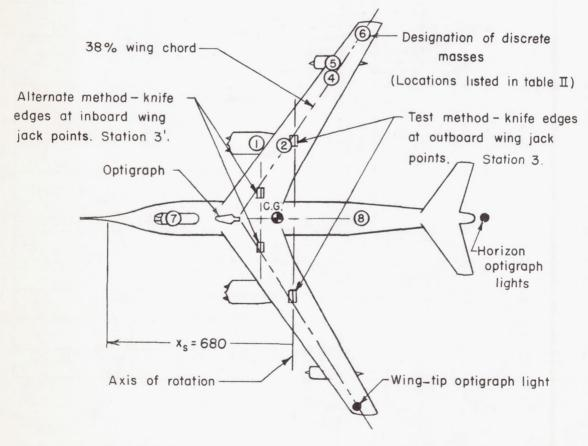
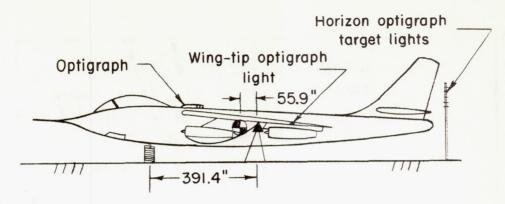
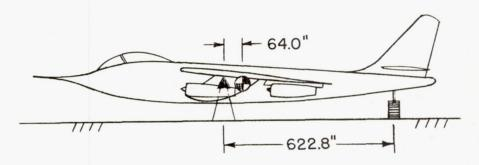


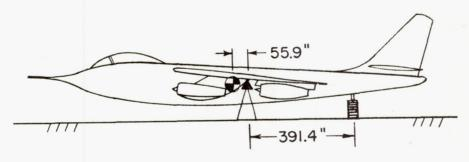
Figure 2.- Plan view of test airplane and discrete masses.



(a) Knife edges at outboard wing jack points and compression spring at forward fuselage jack point.



(b) Knife edges at inboard wing jack points and compression spring at aft fuselage jack point.



(c) Knife edges at outboard wing jack points and tension spring aft of pivot.

Figure 3.- Test airplane supported on knife edges and springs at various locations.

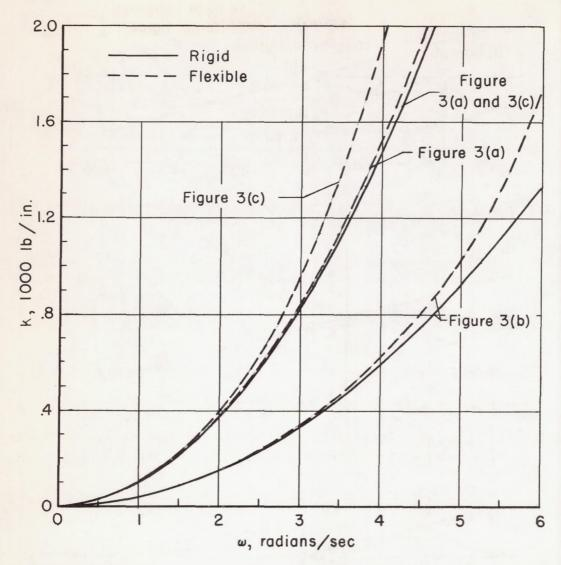
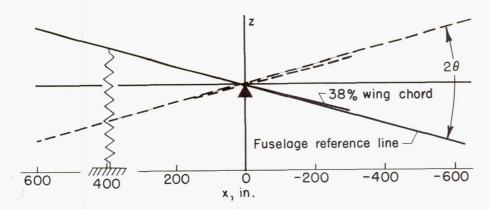
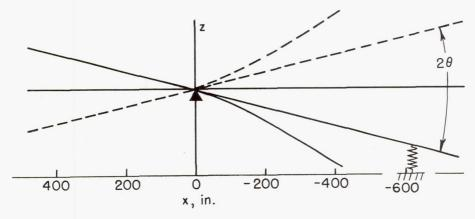


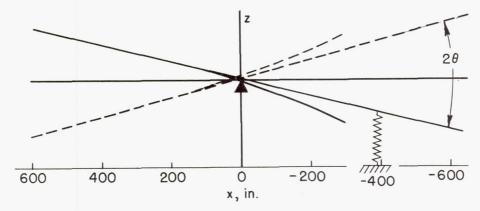
Figure 4.- Effect of wing bending flexibility on the measured frequency for the various suspension systems in figure 3. (Wing first-bending mode frequency = 7.3 radians/sec.)



(a) Knife edges at outboard wing jacks; spring forward.



(b) Knife edges at inboard wing jacks; spring aft.



(c) Knife edges at outboard wing jacks; spring aft.

Figure 5.- Fundamental modes for spring-knife-edge arrangements shown in figure 3 (k = 1.132).

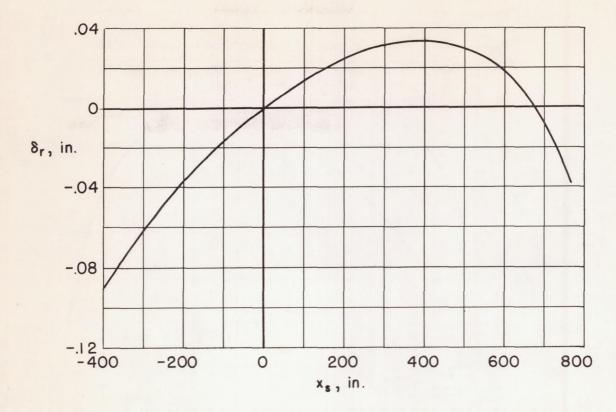


Figure 6.- Deflection of fuselage relative to knife-edge axis for various spring locations and 1-inch deflection at station 7. (Knife edges at outboard wing jacks.) (k = 1.132)

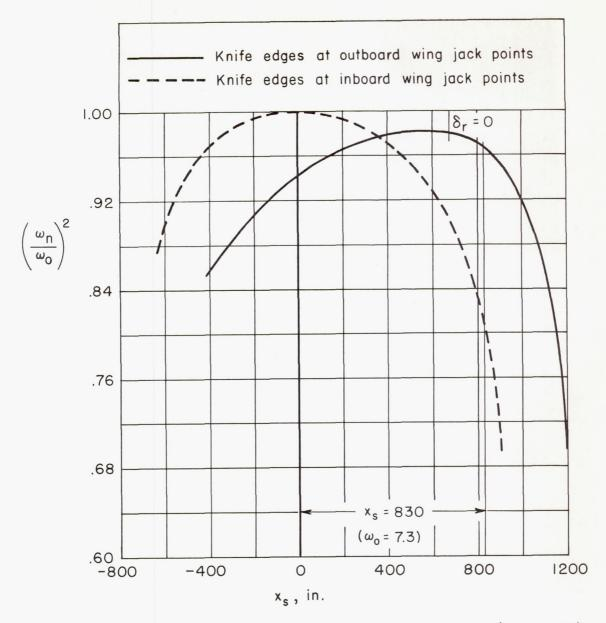
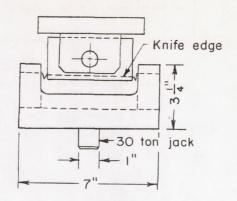


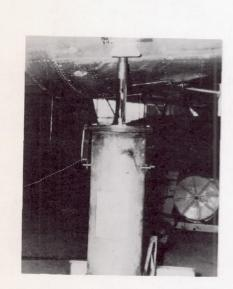
Figure 7.- Effect of spring location on inertia parameter (k = 1.132).



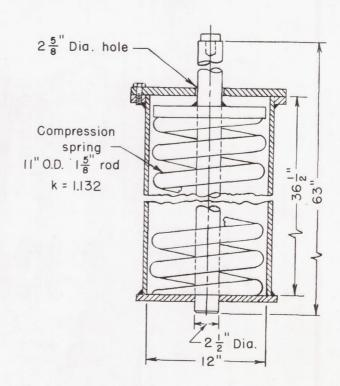


A-2024

(a) Knife-edge installation.



A-20240



(b) Spring installation.

Figure 8.- Knife-edge and spring details.

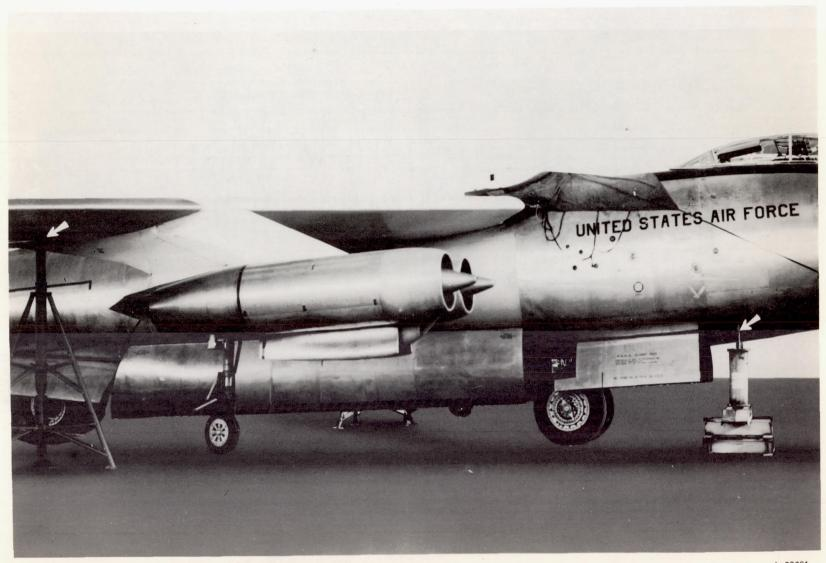


Figure 9.- Photograph of spring and knife-edge installation.

A-20691

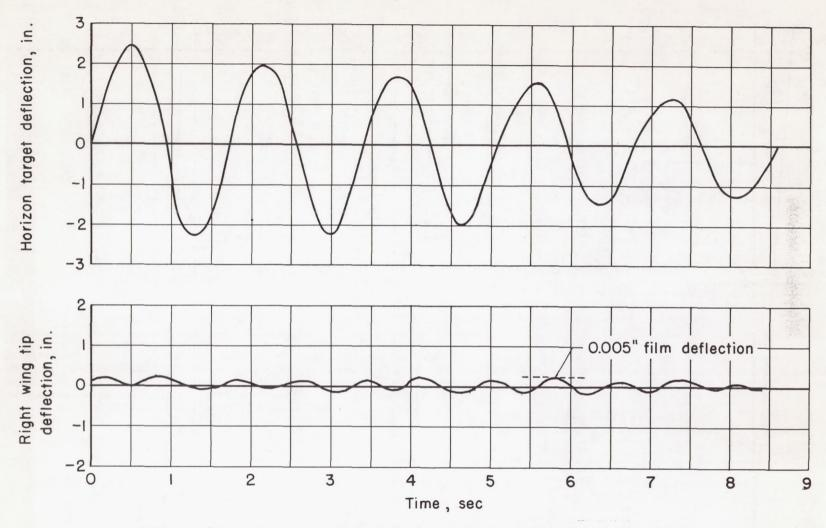
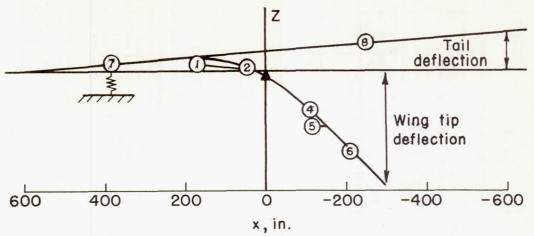
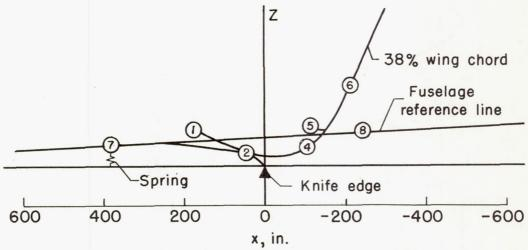


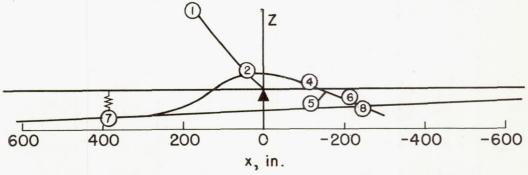
Figure 10.- Time histories of horizon target deflection and wing-tip deflection.



First subdominant mode ( $\omega_n$  = 8.62 radians/sec).



Second subdominant mode ( $\omega_n = 16.18 \text{ radians/sec}$ ).



Third subdominant mode ( $\omega_n = 23.66 \text{ radians/sec}$ ).

Figure 11.- Calculated subdominant modes for test configuration.